

Effect of Ion Irradiation on Mechanical Behaviors of $\text{Ti}_{40}\text{Zr}_{25}\text{Be}_{30}\text{Cr}_5$ Bulk Metallic Glass

Zheng Hu^a, Ziqiang Zhao^b, Yanping Hu^a, Jianshuo Xing^a, Tong Lu^a, Bingchen Wei^{a*}

^aKey Laboratory of Microgravity, National Microgravity Laboratory, Institute of Mechanics,
Chinese Academy of Sciences, 100190, Beijing, China

^bKey Laboratory of Heavy Ion Physics, Ministry of Education, Institute of Heavy Ion Physics,
Peking University, 100871, Beijing, China

Received: December 7, 2011; Revised: March 15, 2012

In this work, the effect of C^{4+} and Cl^{4+} ion irradiation with 25 MeV energy on the hardness and shear banding feature of $\text{Ti}_{40}\text{Zr}_{25}\text{Be}_{30}\text{Cr}_5$ bulk metallic glass was studied. Depth-sensing nanoindentation and microindentation were applied for characterizing the multiple-scaled hardness and shear band patterns during plastic deformation. It is shown that the Cl^{4+} ion irradiation leads to an obvious softening of the sample surface, and distinctly affects the serrated flow feature during plastic deformation. In contrast, C^{4+} ions have little effect on the hardness and shear band patterns. Besides, the mechanism for the change of the mechanical properties and plastic deformation behavior after ion irradiation was also discussed.

Keywords: bulk metallic glass, ion irradiation, indentation, shear bands, hardness

1. Introduction

Nowadays, the development of ion irradiation technologies has ascended to a new level. The interest in both research and industrial areas is aroused by the possibility of modifying physical and chemical properties of materials, even on the nanometer scale, either through the energy deposition by the ions and/or by the implanted ion species themselves. Incident ions lose their energy in solids predominantly via two mechanisms. First, a direct transfer of kinetics energy to target atoms by elastic collisions between a projectile nucleus and target nuclei is commonly denoted as nuclear energy loss S_n . Energy is also transferred to target electrons by the generation of electronic excited or ionized target atoms, which is called electronic energy loss S_e that contributes the most to the energy loss of ions with energy above 0.1 MeV.u⁻¹[1]. In crystalline metals and alloys, it is well known that ion irradiation leads to severe modifications of the structure through the formation of self-interstitials, vacancy loops and transmutation. Due to their inherent disordered structure, metallic glasses are supposed to be resistant against displacive irradiation. For this reason, these materials are potential candidates for applications in irradiation environments, such as fusion, spallation sources, etc. Many works on the thin film metallic glasses have also been carry out, where nanocrystallization and macroscopic anisotropic growth effect etc. have been reported²⁻⁷. Furthermore, in metallic glasses, target atoms will be displaced from their initial sites upon energetic ion irradiation, which may create vacancy-like defects and even could modify the local atomic structure. This provides a possible route for improving the ductility of metallic glasses. Therefore, the effect of ion irradiation on the mechanical properties in bulk metallic glasses (BMGs) has also been

reported. Significant reduction in strength has been found in a Ni ion irradiated $\text{Zr}_{41.2}\text{Ti}_{13.8}\text{Cu}_{12.5}\text{Ni}_{10}\text{Be}_{22.5}$ BMG, which was explained with the enhancement in the free-volume content⁸. However, in other works, distinct surface hardening in $\text{Zr}_{55}\text{Cu}_{30}\text{Ni}_5\text{Al}_{10}$ irradiated by Co^{19} or Ar^{10} ions was demonstrated, which was attributed to the denser packing structures formed under ion irradiation. Therefore, the irradiation effects in BMGs and their underlying mechanism are still unclear. In this work, $\text{Ti}_{40}\text{Zr}_{25}\text{Be}_{30}\text{Cr}_5$ BMG was irradiated by C^{4+} and Cl^{4+} ions, respectively. Hardness and deformation behavior of the BMG were studied by using depth-sensing nanoindentation. Furthermore, subsurface deformation morphology of as-cast and irradiated samples was also investigated by using the bonded interface technique¹¹.

2. Experimental Methods

Cylinders of $\text{Ti}_{40}\text{Zr}_{25}\text{Be}_{30}\text{Cr}_5$ alloy with 5 mm diameter were prepared by arc melting and suction casting under pure argon atmosphere. The amorphous structure of the samples was confirmed by X-ray diffraction (XRD) using $\text{Cu K}\alpha$ radiation. Before irradiation, some $3 \times 3 \times 10$ mm rectangular blocks were cut from the cylindrical samples by using a linear cutting machine and polished with standard metallographic techniques to an exact desired finish for the sake of ion irradiation. The irradiation experiments were performed by 25 MeV C^{4+} and Cl^{4+} ions to the polished surface using a 2×6 MV tandem accelerator. During ion irradiation the sample holders were cooled by a liquid nitrogen cooling system. The irradiation fluence is 9.60×10^{14} cm⁻² for C^{4+} ions and 7.63×10^{15} cm⁻² for Cl^{4+} ions, respectively.

*e-mail: weibc@imech.ac.cn

Nanoindentation measurements were performed in a MTS Nano Indenter® XP with a Berkovich tip and a cube-corner tip, respectively. The former tip is employed for standard hardness and modulus measurements using continuous stiffness method, while the latter is used for highlighting the serration flow phenomenon^{12,13}. The subsurface deformation morphology was checked through microindentation using the bonded interface technique, wherein the irradiated surface and un-irradiated surface were bonded together for comparison. The morphology of the plastic deformed region after indentations was observed by a JSM-6460 scanning electron microscope (SEM).

3. Results and Discussion

XRD patterns obtained from the as-cast and irradiated $\text{Ti}_{40}\text{Zr}_{25}\text{Be}_{30}\text{Cr}_5$ BMGs are shown in Figure 1. The as-cast specimen consists of only one broad diffraction peak without any sharp Bragg peaks, indicating its amorphous structure. For the ion irradiated samples, the XRD spectrums also show one broad diffraction peak, which indicates that the BMGs still maintain an amorphous structure after irradiation.

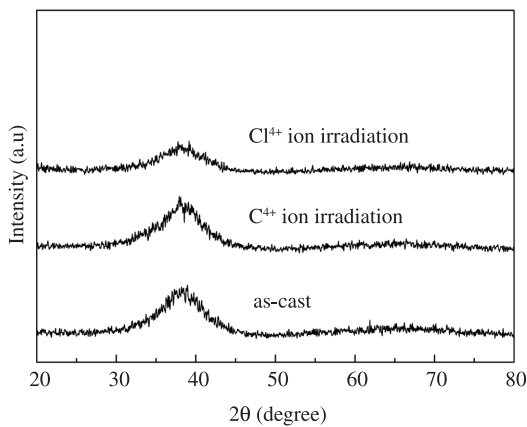


Figure 1. XRD patterns of the BMG before and after ions irradiation.

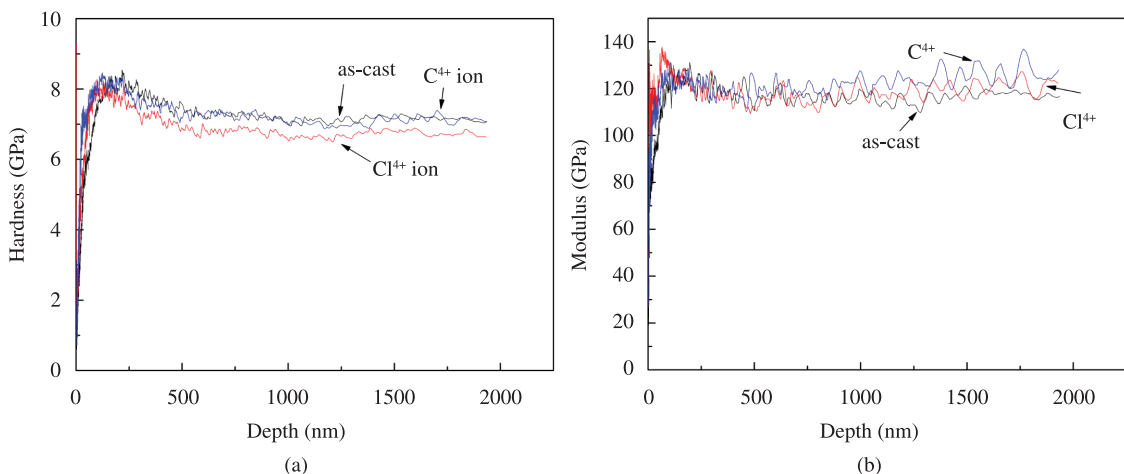


Figure 2. Plots of the hardness (a) and the elastic modulus (b) of as-cast and irradiated BMG samples versus contact depth obtained from nanoindentation.

The projected range and displacement damage (displacement per atom, dpa) are calculated using SRIM code¹⁴. C^{4+} and Cl^{4+} ion irradiated samples on the present BMG produces the maximum displacement damage value of 0.1 and 5.7 dpa, respectively. Furthermore, the region of the most severe radiation damage is well correlated to the mean projected range. For C^{4+} and Cl^{4+} ion irradiation, the mean projected ranges are approximately 15.8 and 5.26 μm , respectively, below the samples surface. It should be noted that the displacement damage induced by Cl^{4+} ion irradiation is more severe than that of C^{4+} ions, while the mean projected range is lower, because of its high atomic number.

From the calculated results by SRIM, we know that ion irradiation with high ion fluence can cause damage on the surface layer of samples. Nanoindentation was used to study the effect of irradiation on hardness and modulus of the BMGs. The profiles of hardness and modulus as a function of probing depth for as-cast, C^{4+} ion and Cl^{4+} ion irradiated samples are shown in Figure 2. It is obvious that the hardness of the Cl^{4+} ion irradiated sample is lower than that of the as-cast sample, while the C^{4+} ion irradiated sample exhibits a similar hardness with the as-cast one throughout the whole indentation depth range (Figure 2a). The average hardness value of the as-cast, C^{4+} ion irradiated and Cl^{4+} ion irradiated sample is 7.18, 7.16 and 6.74 GPa, respectively. This indicates a significant softening by severe Cl^{4+} ion irradiation damage (5.7 dpa), while the relative weak damage (0.1 dpa) caused by C^{4+} ion irradiation does not change the hardness of the sample. The modulus values of the as-cast, C^{4+} ion irradiated and Cl^{4+} ion irradiated samples are almost the same throughout the penetration process of nanoindentation (Figure 2b). The average modulus values for all these three samples are about 118 GPa. This indicates that irradiation damage in the present study does not change the modulus of the BMG.

In order to explore the effect of ion irradiation on the plastic deformation behavior of the BMGs, nanoindentation measurements with cube-corner tip were made on the as-cast and irradiated samples. Compared with the Berkovich tip at the same load level, the sharper cube-corner tip can produce a larger peak-load displacement and a greater

proportion of permanent plastic deformation after unloading. Typical load-displacement (P-h) curves at the loading rate of 16.7 mN/s are presented in Figure 3a. In this figure the origin of each curve has been displaced so that multiple curves can be seen clearly on the graph, and only the loading portions of the P-h curves are shown for clarity. Again, the significant softening can be found in the Cl^{4+} ion irradiated sample, while the C^{4+} ion irradiated sample shows comparable hardness with the as-cast sample. Furthermore, pronounced serrated flow during the loading process of nanoindentation can be found in all these three samples. In order to demonstrate the characteristics of this serrated flow clearly, these P-h curves were fitted with smooth power law function^{15,16}: $P_{\text{fit}} = K \times h^m$, where K and m are the loading rate-dependent fitting constants. For a given penetration depth h, the corresponding loads P_{fit} can be determined using this function, whereas the corresponding experimental values of loads, P_{exp} , can be obtained from the curves illustrated in Figure 3a. Obviously, the amount $\Delta P = P_{\text{exp}} - P_{\text{fit}}$ can show the deviation of the load during loading process. The ΔP -h curves of the three samples during nanoindentation are shown in Figure 3b. It can be seen that the oscillation magnitude of the load deviation ΔP of the as-cast sample is higher than that of the two irradiated samples. It is also remarkable that the oscillation

magnitude of irradiated samples are more irregular and the number of small values of ΔP increases, especially in the Cl^{4+} irradiated sample. It demonstrates that ion irradiation changes the serrated flow feature from a regular serration in the as-cast sample to irregular behavior in the Cl^{4+} and C^{4+} ion irradiated samples. Typical morphology of the plastic deformation region around the indent after nanoindentation is shown in Figure 3c. Though numbers of shear bands can be found around the indents, they could not provide enough information on the effect of irradiation on the operation feature of shear band, due to the fact that the ever damage layer just occupies a small portion of the whole plastic deformation region.

For further clarifying the shear band patterns affected by the ion irradiation, the subsurface deformation morphology was checked through microindentation using the bonded interface technique, wherein the irradiated surface and un-irradiated surface were bonded together for a good comparison. In this case, the whole deformation region on the interface has undergone ion irradiation. Typical SEM images for the plastic deformation region underneath the indents are shown in Figure 4. For the as-cast sample, there are principally two sets of shear bands, semicircular and radical, and the former type is dominating (Figure 4a). The radical shear bands intersect the semicircular shear

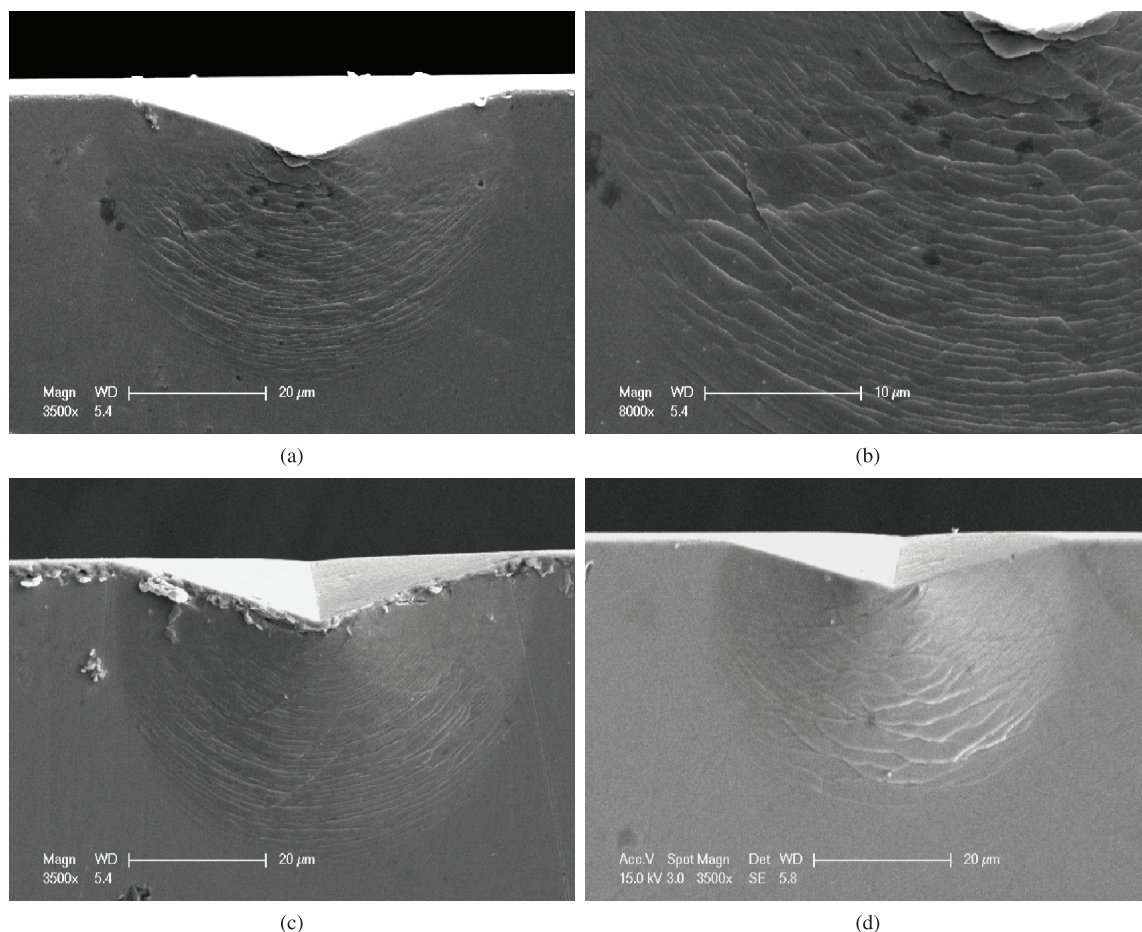


Figure 4. Morphology of shear band patterns underneath indents after indentation with the bonded interface technique: (a) as-cast BMG, (b) higher magnification image of (a), (c) C^{4+} ion irradiated BMG, (d) Cl^{4+} ion irradiated BMG.

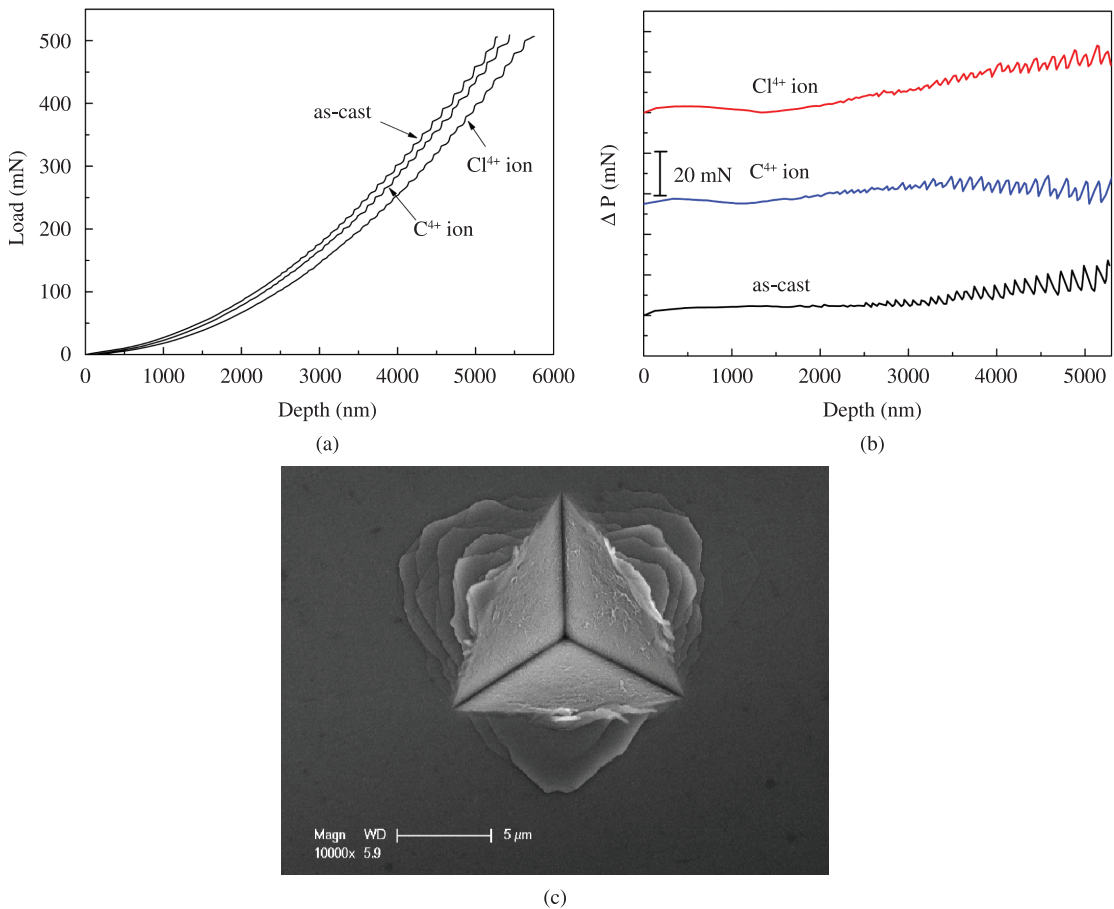


Figure 3. a) Load-depth curves during nanoindentation for the as-cast and irradiated samples; b) Load deviation-depth curves for the as-cast and irradiated samples; c) Typical morphology of the plastic deformation region around the indent after indentation with Cube-corner tip.

bands and leave small shear-offsets behind (Figure 4b). The shear band patterns of the C⁴⁺ ion irradiated sample (Figure 4c) are quite similar to that of the as-cast sample. These two sets of shear bands can also be identified in the deformed zone and the number of the semi-circular shear bands is larger than that of the radical shear bands. The shear band patterns of Cl⁴⁺ irradiated sample are shown in Figure 4d. In this figure we could also see a hemispherical deformation zone. However, the shear band patterns are more complex and disordered than those in as-cast sample. The characteristics of semi-circular shear bands are branching and discontinuous. Besides, the spacing between shear bands is larger in the area just below the indenter tip. The above results demonstrate that the shear band patterns would change when suffering severe irradiation damage by heavy ions.

Under MeV ion irradiation, the density of electronic excitations and ionization becomes so high that new unexpected and collective effects arise. Violent nucleus-nucleus collisions can create displacement cascade and thermal spikes, which leaves some defects like vacancy rich, nanocrystal, melting and resolidification in solids¹⁷. It is possible that amorphous alloys, being metastable, may crystallize on irradiation. However, distinct crystallization upon irradiation does not take place within the detect limit

of XRD in this work. Therefore, the possible mechanism of damage process is that when ions are implanted into the surface of BMG, target atoms will be displaced from their initial sites, especially at high energy transfer. This creates vacancy-like defects and increases excessive free volume in the system. Through the results of nanoindentation experiments, it can be found that there is obvious softening on the ion irradiated BMG, especially for the Cl⁴⁺ ion irradiated sample, with the hardness decreased by about 6%. The softening is related to the increase in free volume or defects in atomic scale, which is also in accordance with the free volume theory^{18,19}.

As shown in Figure 3 and Figure 4, the serrated flow phenomenon during the plastic deformation become more irregular in ion irradiated samples, and the shear band patterns beneath the indents of irradiated samples also change from a relatively regular distribution in the as-cast sample to a disordered feature in the Cl⁴⁺ ion irradiated sample. These phenomena further verify that the formation and propagation of shear bands are indeed disrupted by ion irradiation, due to the introduction of excess randomly distributed defects or local atomic structural changes by ion irradiation. This also changes the stress distribution at the shear band tip during its propagation, giving rise to a deviation of shear band from their original direction

during the plastic deformation of the BMG. Therefore, shear band patterns in the irradiated samples tends to be a disordered and branching feature, and the serrated flow feature becomes more irregular. The above results also suggest that ion irradiation could be a possible technique to improve the plasticity of BMG, due to the introduction of excess atomic-scale defects and the change of the mode of shear band propagation.

4. Conclusions

The effect of C⁴⁺ and Cl⁴⁺ ion irradiation on mechanical behaviors of Ti₄₀Zr₂₅Be₃₀Cr₅ BMG was studied. Irradiation damage to the samples is about 5.7 dpa, corresponding damage peak depth of about 5.26 μm by Cl⁴⁺ ions, while 0.1 dpa damage, 15.8 μm depth by C⁴⁺ ions, respectively.

It is found that BMG still maintain an amorphous structure after high energy heavy ions irradiation. C⁴⁺ ion irradiation, producing low irradiation damage, does not change the mechanical behavior of the BMG. However, Cl⁴⁺ irradiation decreases the hardness of the surface layer of BMG, and distinctly alters the serrated flow feature and shear band patterns during plastic deformation. The change of the deformation behavior is attributed to the introduction of excess atomic-scale defects by ion irradiation.

Acknowledgements

This work is financially supported by the National Nature Science Foundation of China (Grant Nos. 51071166 and 10675010) and National Basic Research Program of China (973 Program, No. 2010CB832902 and 2010CB832904).

References

- Trautmann C, Toulemonde M, Dufour C and Paumier E. Effect of radial energy distribution on ion track etching in amorphous metallic Fe₈₁B_{13.5}Si_{3.5}C₂. *Nuclear Instruments & Methods in Physics Research Section B-Beam Interactions with Materials and Atoms*. 1996; 108(1-2):94-98. [http://dx.doi.org/10.1016/0168-583X\(95\)00857-8](http://dx.doi.org/10.1016/0168-583X(95)00857-8)
- Narayan H, Agrawal HM, Kushwaha RPS, Kanjilal D and Sharma SK. Surface smoothing of metallic glasses by swift heavy ion irradiation. *Nuclear Instruments & Methods in Physics Research Section B-Beam Interactions with Materials and Atoms*. 1999; 156(1-4):217-221. [http://dx.doi.org/10.1016/S0168-583X\(99\)00265-7](http://dx.doi.org/10.1016/S0168-583X(99)00265-7)
- Nagase T and Umakoshi Y. Electron irradiation induced nanocrystallization behavior in Fe₇₁Zr₉B₂₀ metallic glass. *Materials Transactions*. 2005; 46(3):608-615. <http://dx.doi.org/10.2320/matertrans.46.608>
- Nino A, Nagase T and Umakoshi Y. Electron irradiation induced nano-crystallization in Fe₇₇Nd_{4.5}B_{18.5} metallic glass. *Materials Transactions*. 2005; 46(8):1814-1819. <http://dx.doi.org/10.2320/matertrans.46.1814>
- Nagase T, Nakamura M and Umakoshi Y. Electron irradiation induced nano-crystallization in Zr_{66.7}Ni_{33.3} amorphous alloy and Zr₆₀Al₁₅Ni₂₅ metallic glass. *Intermetallics*. 2007; 15(2):211-224. <http://dx.doi.org/10.1016/j.intermet.2006.05.009>
- Umakoshi Y and Nagase T. Electron irradiation induced phase transformation of supercooled liquid and amorphous phases in Zr_{66.7}Cu_{33.3} metallic glass. *Materials Science and Engineering A-structural Materials Properties Microst*. 2007; 449:605-608.
- Klaumunzer S and Schumacher G. Dramatic Growth of Glassy Pd₈₀Si₂₀ during Heavy-Ion Irradiation. *Physical Review Letters*. 1983; 51(21):1987-1990. <http://dx.doi.org/10.1103/PhysRevLett.51.1987>
- Raghavan R, Boopathy K, Ghisleni R, Pouchon MA, Ramamurty U and Michler J. Ion irradiation enhances the mechanical performance of metallic glasses. *Scripta Materialia*. 2010; 62(7):462-465. <http://dx.doi.org/10.1016/j.scriptamat.2009.12.013>
- Yang YZ, Tao PJ, Li GQ, Mu ZX, Ru Q, Xie ZW et al. Effects of ion implantation on surface structures and properties for bulk metallic glass. *Intermetallics*. 2009; 17(9):722-726. <http://dx.doi.org/10.1016/j.intermet.2009.02.013>
- Iqbal M, Akhter JI, Hu ZQ, Zhang HF, Qayyum A and Sun WS. Mechanical properties and ion irradiation of bulk amorphous Zr₅₅Cu₃₀Al₁₀Ni₅ alloy. *Journal of Non-Crystalline Solids*. 2007; 353(24-25):2452-2458. <http://dx.doi.org/10.1016/j.jnoncrysol.2007.04.013>
- Ramamurty U, Jana S, Kawamura Y and Chattopadhyay K. Hardness and plastic deformation in a bulk metallic glass. *Acta Materialia*. 2005; 53(3):705-717. <http://dx.doi.org/10.1016/j.actamat.2004.10.023>
- Jang JI, Lance MJ, Wen SQ, Tsui TY and Pharr GM. Indentation-induced phase transformations in silicon: influences of load, rate and indenter angle on the transformation behavior. *Acta Materialia*. 2005; 53(6):1759-1770. <http://dx.doi.org/10.1016/j.actamat.2004.12.025>
- Jang JI, Lance MJ, Wen SQ and Pharr GM. Evidence for nanoindentation-induced phase transformations in germanium. *Applied Physics Letters*. 2005; 86(13):131907. <http://dx.doi.org/10.1063/1.1894588>
- Pavlovic M and Strasik I. Supporting routines for the SRIM code. *Nuclear Instruments & Methods in Physics Research Section B-Beam Interactions with Materials and Atoms*. 2007; 257:601-604. <http://dx.doi.org/10.1016/j.nimb.2007.01.047>
- Zeng K and Chiu CH. An analysis of load-penetration curves from instrumented indentation. *Acta Materialia*. 2001; 49(17):3539-3551. [http://dx.doi.org/10.1016/S1359-6454\(01\)00245-2](http://dx.doi.org/10.1016/S1359-6454(01)00245-2)
- Ma X, Yoshida F and Shinbata K. On the loading curve in microindentation of viscoplastic solder alloy. *Materials Science and Engineering A-structural Materials Properties Microst*. 2003; 344(1-2):296-299.
- Nastasi MA, Mayer JW and Hirvonen JK. *Ion-solid interactions: fundamentals and applications*. Cambridge: Cambridge University Press; 1996. 540 p.
- Spaepen F. Microscopic Mechanism for Steady-State Inhomogeneous Flow in Metallic Glasses. *Acta Metallurgica*. 1977; 25(4):407-415. [http://dx.doi.org/10.1016/0001-6160\(77\)90232-2](http://dx.doi.org/10.1016/0001-6160(77)90232-2)
- Heggen M, Spaepen F and Feuerbacher M. Creation and annihilation of free volume during homogeneous flow of a metallic glass. *Journal of Applied Physics*. 2005; 97(3). <http://dx.doi.org/10.1063/1.1827344>